JOURNAL OF COMPUTATIONAL PHYSICS 119, 342–355 (1995)

# Electromagnetic Scattering from Dielectrically Coated Axisymmetric Objects Using the Generalized Point-Matching Technique

## I. Theoretical Formulation

H. M. AL-RIZZO AND J. M. TRANQUILLA

*Radiating Systems Research Laboratory, Department of Electrical Engineering, University of New Brunswick, Fredericton, New Brunswick, Canada E3B 5A3*

Received May 25, 1994

This paper presents a general and systematic numerical technique based upon the generalized point-matching technique (GPMT) for analyzing problems of plane electromagnetic (EM) scattering from three-dimensional bounded objects consisting of (or modelled by) an arbitrarily shaped axisymmetric perfectly conducting or dielectric obstacle embedded in an arbitrarily shaped dielectric body of revolution and arbitrarily disposed with respect to the propagation direction of an arbitrarily polarized incident electric field vector. The GPMT has the chief advantage of being conceptually simple and is amenable to solution by numerical techniques without excessive analytical and/or programming effort. The treatment may be validly applied to scatterers whose boundary surfaces must have no sharp corners or edges which will introduce a discontinuity in the direction of the unit vector normal to the core and/or outer coat surfaces. However, it should be pointed out that when applicable, the method is remarkably robust and capable of providing highly accurate numerical modelling predictions for the full-vector EM wave interactions with a large variety of arbitrarily shaped two-layered structures. 

### I. INTRODUCTION

The first reported case of electromagnetic (EM) scattering by a finite, 3D inhomogeneous object for which an analytical closed-form solution has been obtained is the two-layered, concentric spherical structure of dissimilar material properties [1]. Since 1951, various new computational techniques have emerged in numerical electromagnetics, which make it possible to treat scattering from arbitrarily shaped, 2- and 3D inhomogeneous objects comprising perfectly conducting (PC), dielectric, and anisotropic materials. The T-matrix formulation, developed originally by Waterman [2, 3] for the case of EM scattering by homogeneous PC and dielectric scatterers has been extended by Peterson and Ström [4] to include scattering from objects consisting of an arbitrary number of consecutively enclosing surfaces. Bringi and Seliga [5, 6] utilized the formulation of Peterson and Ström [4] to calculate the radar cross sections (RCSs) for both PC and dielectric obstacles embedded within another dielectric body. The coupled-dipole method, developed originally by Purcell and Pennypacker [7] to approximate light scattering by a particle of arbitrary shape has been extended by Druger *et al.* [8] to analyze scattering by inhomogeneous particles. However, the method does not appear to be feasible, at present, to treat scattering by particles of large size parameters and/or permittivities. Pogorzelski [9] presented an efficient and quite general formulation to the problem of EM scattering from inhomogeneous penetrable objects in order to overcome the matrix-size difficulties frequently encountered in the surface integral-equation (SIE) method for particles of large electrical size.

The method of moments (MoM), developed by Mautz and Harrington [10], has been generalized by Medgyesi-Mitschang and Eftimiu [11] to treat scattering from axisymmetric bodies embedded in axisymmetric dielectrics. Wang and Barber [12] applied the extended boundary-condition method (EBCM) to EM scattering by water-coated hailstones and small chemical and biological particles. The problem of EM scattering from PC, rotationally symmetric bodies coated with lossless homogeneous dielectrics was investigated by Kishk and Shafai [13] using a SIE method. The equivalence principle was invoked to generate seven different formulations which were subsequently reduced to matrix equations using the MoM. Morgan *et al.* [14] developed a hybrid method of EM scattering from inhomogeneous, axisymmetric penetrable bodies. Their formulation combines the robust capabilities of the finite element method (FEM) in modelling complicated internal inhomogeneous dielectric structures and the SIE formulation embodied in the EBCM. Yuan *et al.* [15] demonstrated the validity and accuracy of a hybrid formulation, which combines the MoM when treating the unbounded scattering problem and the suitability of the FEM in handling complex internal inhomogeneities. Finally,



0021-9991/95 $12.00

Sebak and Sinha [16] presented an analytical solution, based on separating the vector wave equation in spheroidal coordinates, for scattering of a plane EM wave by PC spheroids coated with a dielectric material, for axial incidence.

It is worth mentioning, however, that each of the above-mentioned techniques has its own range of applicability and is suitable only for certain ranges of parameters depending on the scatterer shape, EM constitutive parameters and scatterer size relative to the wavelength of the incident radiation. Consequently, a single generic computer program capable of addressing all of the possible and highly diversified applications has not been available.

One of the main objectives of the present paper is the development of a general and systematic semi-analytical approach based on the analytical solutions of Maxwell's equations in terms of spherical vector wavefunction expansions combined with the generalized point-matching technique (GPMT) as a tool for analyzing the EM scattering characteristics of a broad hierarchy of arbitrarily shaped, 3D axisymmetric PC or dielectric obstacles encased in a lossy dielectric shell of a second material, when the scattering object is at an arbitrary orientation with respect to the direction of propagation of an arbitrarily polarized incident plane EM wave. While the analytical formulations provided can be easily generalized to arbitrarily shaped 3D scattering objects, only the special category of convex/concave bodies of revolution has been considered here because of their physical significance. The techniques developed here, which are conceptually simple and amenable to solutions by numerical techniques without excessive analytical and/or programming effort, have resulted in the development of a highly accurate and versatile computer code [17] that can be used in a wide variety of applications in areas of current research interest such as designing and testing of absorbing materials used to minimize the effects of structures involved in RCS measurements, radar camouflage, interpretation of polarimetric radar signals for determining the morphology of dry and wet hydrometeors and predicting the potential health hazards of non-ionizing radio-frequency radiation.

## II. OUTLINE OF THE GPMT

The basis for establishing the theoretical formulation of the point-matching technique (PMT) is based upon the assumption that the entire relevant domain of the scattering problem may be divided into a number of separate homogeneous regions of different material properties. The solution to the vector wave equation is determined in each region, subject to the appropriate boundary conditions on the boundaries common to any two different regions.

As the name implies, the PMT refers in general to the numerical procedure in which the boundary conditions are satisfied only at a finite number of appropriately selected points on the interfacial surfaces separating regions of different constitutive parameters. The PMT has been previously employed in the numerical solution of 2D problems of EM scattering by either PC cylinders of infinite length [18], or by infinitely long, dielectric-coated PC cylinders [19], both of arbitrary but smooth cross sections. The method has also been applied to EM scattering by finite, 3D homogeneous PC and lossy dielectric objects, including spheres and spheroids with small eccentricities [20–22]. To the best of the authors' knowledge, the PMT has not yet been extended to 3D, axisymmetric multilayered dielectric objects.

The analytical formulation of the PMT begins by expanding the scattered field exterior to the scatterer and the transmitted fields induced internally in each layer by doubly-infinite series involving linear combinations of basic spherical vector wavefunctions, which are the fundamental set of solutions to the vector wave equation in spherical polar coordinates.

An obliquely incident, time-harmonic, plane wave of arbitrary polarization is assumed for the exciting field. The mathematical description of the two linearly polarized components of the incident wave can be accomplished easily in rectangular coordinates. However, a complex azimuthal Fourier decomposition is chosen for the two orthogonal linear polarizations in order to facilitate the removal of the azimuthal dependence appearing in the spherical vector wavefunctions. Computational simplification occurs since the azimuthal and elevation modal indices can be partially decoupled in the final boundary-condition equations.

The infinite modal summations for the incident, scattered and internal fields are truncated in the numerical computations at some finite modal indices, depending upon the accuracy desired in the final solution. The boundary conditions, which require in general the continuity of the tangential components of the total electric and magnetic field vectors across the boundaries, are then applied to the truncated field expansions leading, in general, to four independent scalar equations for each bounding layer. Collocation or, equivalently, simple point matching may be used to formulate the necessary number of independent, simultaneous linear equations by successively choosing representative points on the surface at which the boundary conditions are exactly satisfied. Because of the axial symmetry involved, each matching point corresponds to a circle around the axis of rotational symmetry. However, it should be emphasized that the boundary conditions may not be exactly satisfied at points which are not explicitly included in the point-matching procedure.

Another approach, referred to as the GPMT [21–24], is achieved by selecting a number of matching points which is typically larger than twice the number of unknown expansion coefficients for the scattered field, and the boundary conditions are then satisfied in the least-squares error sense. This approach has the advantages of improving the numerical stability, reducing the average and maximum errors in the overall boundary fit and, finally, the dependence of the final solution on the particular selection of field matching points is significantly relaxed [24, 25].

Once the unknown expansion coefficients have been determined, the truncated expansions of the scattered and internal fields can be utilized to provide an approximate solution for the complete scattering problem.

## III. THEORETICAL DEVELOPMENT

### 1. *Statement of the Problem*

In order to develop a theoretical formulation applicable to scatterers arbitrarily oriented with respect to the propagation and polarization directions of the incident wave, two frames of reference will be introduced, a discussion of which is reserved until Subsection 6. Since only rotationally symmetric objects are considered, it is often convenient to solve the scattering problem in a coordinate system coincident with the natural axes of the scatterer.

An arbitrarily shaped, two-layered, axisymmetric body excited by an obliquely incident plane wave is depicted in Fig. 1. The right-handed rectangular coordinate system $(x, y, z)$, attached to the set of natural axes of the scatterer, will be referred to as the local frame. The origin of this frame is located at the center of the scatterer, corresponding to the point of maximum symmetry. This will facilitate the utilization of the rotational symmetry of the scatterer whereby the original 3D problem can be reduced later to a series of 2D ones.

The scattering volume is bounded by closed surfaces $S_1$ and $S_2$, where $S_2$ encloses $S_1$. It is assumed hereafter that $S_1$ and $S_2$ are sufficiently smooth that the divergence theorem is applicable and that the scatterer has no sharp corners or edges. Accordingly, continuous, single-valued, outward-pointing unit normal vectors $\hat{\mathbf{n}}_1$ and $\hat{\mathbf{n}}_2$ are defined at each point on $S_1$ and $S_2$. The volume enclosed by $S_1$ is called the core region, which can be either a PC or a lossy dielectric with constitutive parameters $\mu_{r1}$ and $\varepsilon_{r1}$, where $\mu_{r1}$ is the relative permeability and $\varepsilon_{r1}$ is the relative permittivity of the dielectric material. The shell region, bounded by $S_1$ and $S_2$, is characterized by the parameters $\mu_{r2}$ and $\varepsilon_{r2}$. Without loss of generality, the surrounding medium is considered to be a free-space environment with constitutive parameters $\mu_0$ and $\varepsilon_0$. Since only non-magnetic materials are considered, the permeability is assumed to be uniform throughout the entire space, $\mu_{r2} = \mu_{r1} = 1$.

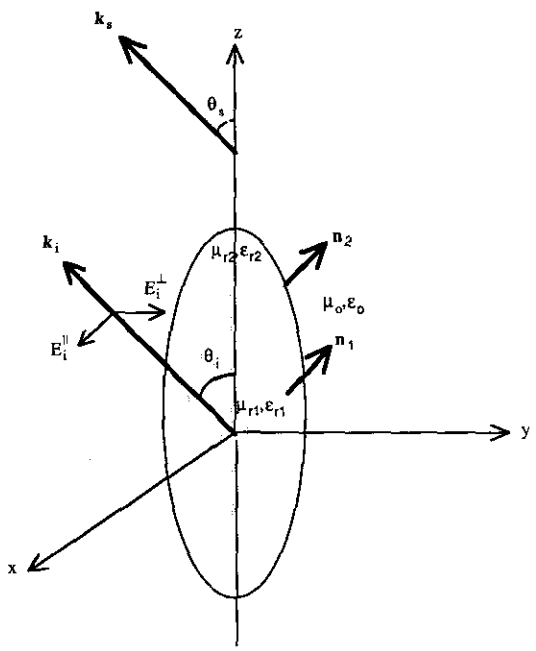


FIG. 1. Geometry for the problem of scattering by a dielectrically coated, three-dimensional axisymmetric scatterer situated in free-space.

The scattering problem consists of finding solutions for the electric and magnetic field vectors in the whole of the relevant domain, which satisfy the vector wave equations and the appropriate boundary conditions across the boundaries of the domain of interest.

As a consequence of the linearity of Maxwell's equations, one can decompose the total EM fields throughout the entire space surrounding the scatterer ($\mathbf{E}_{tot}$, $\mathbf{H}_{tot}$) into the sum of the known field of the incident plane wave ($\mathbf{E}_i$, $\mathbf{H}_i$), and the scattered field ($\mathbf{E}_s$, $\mathbf{H}_s$). The incident field is defined as the field that would exist in the absence of the scattering volume and in the vicinity of the scatterer can be treated as a plane wave. In the case of a dielectric obstacle, the internal field induced inside the scatterer, ($\mathbf{E}_t$, $\mathbf{H}_t$), is the appropriate wave function of interest.

To this end, the solution of the problem is feasible, provided that the boundary conditions

$$\left.\begin{aligned}\hat{\mathbf{n}}_1 \times \mathbf{E}_{t1}(\mathbf{r}) &= \hat{\mathbf{n}}_1 \times \mathbf{E}_{t2}(\mathbf{r})\\ \hat{\mathbf{n}}_1 \times \mathbf{H}_{t1}(\mathbf{r}) &= \hat{\mathbf{n}}_1 \times \mathbf{H}_{t2}(\mathbf{r})\end{aligned}\right\} \mathbf{r} \in S_1 \tag{1}$$

and

$$\left.\begin{aligned}\hat{\mathbf{n}}_2 \times \mathbf{E}_{t2}(\mathbf{r}) &= \hat{\mathbf{n}}_2 \times \mathbf{E}_{tot}(\mathbf{r})\\ \hat{\mathbf{n}}_2 \times \mathbf{H}_{t2}(\mathbf{r}) &= \hat{\mathbf{n}}_2 \times \mathbf{H}_{tot}(\mathbf{r})\end{aligned}\right\} \mathbf{r} \in S_2 \tag{2}$$

are satisfied across the core and shell surfaces, where ($\mathbf{E}_{t1}$, $\mathbf{H}_{t1}$) and ($\mathbf{E}_{t2}$, $\mathbf{H}_{t2}$) are the internal fields induced in the core and shell regions, respectively. If the core region consists of a PC material, (1) reduces to

$$\hat{\mathbf{n}}_1 \times \mathbf{E}_{t2}(\mathbf{r}) = 0. \tag{3}$$

For the boundary at infinity, the electric and magnetic field vectors of the scattered wave must satisfy Sommerfeld's radiation condition which ensures that the scattered wave crossing the boundary of an infinitely large sphere circumscribing the scatterer must resemble the characteristics of an outward travelling, transverse EM wave to terms in the order of $r^{-1}$ [26],

$$\begin{aligned}\lim_{r\to\infty} r[\sqrt{\varepsilon_0/\mu_0}(\hat{\mathbf{a}}_r \times \mathbf{E}_s) - \mathbf{H}_s] &= 0\\ \lim_{r\to\infty} r[\hat{\mathbf{a}}_r \times \mathbf{H}_s + \sqrt{\varepsilon_0/\mu_0}\mathbf{E}_s] &= 0,\end{aligned} \tag{4}$$

where $\hat{\mathbf{a}}_r$ is a unit radial vector along the direction of propagation of the scattered wave and $r$ is the radius of a large concentric sphere enclosing the scatterer.

### 2. *Fourier Series Expansion of the Incident Field*

An arbitrarily polarized, time-harmonic plane incident wave, propagating in the $\mathbf{k}_i$ direction and inclined at an angle $\theta_i$ with respect to the symmetry axis is assumed. The electric field vector of the incident wave is given by

$$\mathbf{E}_i = \hat{\mathbf{p}} E_0 \exp(j\mathbf{k}_i \cdot r), \tag{5}$$

where $\mathbf{k}_i = k_0(\sin\theta_i\hat{\mathbf{a}}_x + \cos\theta_i\hat{\mathbf{a}}_z)$, $\mathbf{r} = x\hat{\mathbf{a}}_x + y\hat{\mathbf{a}}_y + z\hat{\mathbf{a}}_z$, $k_0 = 2\pi/\lambda$ is the free-space propagation constant and $\lambda$ is the wavelength of the incident radiation. The complex unit vector $\hat{\mathbf{p}}$ describes the polarization state of the incident wave.

The incident wave direction and the axis of rotational symmetry define the incident plane. It is convenient to resolve the electric and magnetic field vectors of the incident wave into two linearly polarized components $(\mathbf{E}_i^{\parallel}, \mathbf{H}_i^{\parallel})$ and $(\mathbf{E}_i^{\perp}, \mathbf{H}_i^{\perp})$, which are respectively parallel and perpendicular to the plane of incidence as

$$\begin{aligned} \mathbf{E}_i &= (\hat{\mathbf{a}}_i^{\parallel} E_i^{\parallel} + \hat{\mathbf{a}}_i^{\perp} E_i^{\perp}) \exp(j\mathbf{k}_i \cdot \mathbf{r}) \\ \mathbf{H}_i &= \frac{\mathbf{k}_0}{\omega\mu_0} (\hat{\mathbf{a}}_i^{\perp} E_i^{\parallel} - \hat{\mathbf{a}}_i^{\parallel} E_i^{\perp}) \exp(j\mathbf{k}_i \cdot \mathbf{r}), \end{aligned} \tag{6}$$

where

$$\begin{aligned} \hat{\mathbf{a}}_i^{\parallel} &= \cos\theta_i\hat{\mathbf{a}}_x - \sin\theta_i\hat{\mathbf{a}}_z \\ \hat{\mathbf{a}}_i^{\perp} &= \hat{\mathbf{a}}_y. \end{aligned} \tag{7}$$

Since the scatterer is symmetrical with respect to the azimuthal angle $\phi$, the incident wave can be decomposed into summations of azimuthal modes having an $\exp(jm\phi)$ variation using the azimuthal Fourier-series representation [22]

$$\begin{aligned} \mathbf{E}_i^{\parallel}(r, \theta, \phi) &= \sum_{m=-\infty}^{\infty} \mathbf{e}_m^{\parallel}(r, \theta) \exp(jm\phi) \\ \mathbf{E}_i^{\perp}(r, \theta, \phi) &= \sum_{m=-\infty}^{\infty} \mathbf{e}_m^{\perp}(r, \theta) \exp(jm\phi) \end{aligned} \tag{8}$$

and

$$\begin{aligned} \mathbf{H}_i^{\parallel}(r, \theta, \phi) &= \frac{k_0}{\omega\mu_0} \frac{E_i^{\parallel}}{E_i^{\perp}} \sum_{m=-\infty}^{\infty} \mathbf{e}_m^{\perp}(r, \theta) \exp(jm\phi) \\ \mathbf{H}_i^{\perp}(r, \theta, \phi) &= \frac{-k_0}{\omega\mu_0} \frac{E_i^{\perp}}{E_i^{\parallel}} \sum_{m=-\infty}^{\infty} \mathbf{e}_m^{\parallel}(r, \theta) \exp(jm\phi), \end{aligned} \tag{9}$$

where $\omega$ is the angular frequency in rad/s.

The spectral components, $\mathbf{e}_m^{\parallel}$ and $\mathbf{e}_m^{\perp}$, can be found from

$$\begin{aligned} \mathbf{e}_m^{\parallel}(r, \theta) &= \frac{1}{2\pi} \int_0^{2\pi} \mathbf{E}_i^{\parallel}(r, \theta, \phi) \exp(-jm\phi)\, d\phi \\ \mathbf{e}_m^{\perp}(r, \theta) &= \frac{1}{2\pi} \int_0^{2\pi} \mathbf{E}_i^{\perp}(r, \theta, \phi) \exp(-jm\phi)\, d\phi. \end{aligned} \tag{10}$$

Transforming all the variables and unit vectors from Cartesian to spherical coordinates and utilizing the integral representation for the regular Bessel functions of the first kind [27] the integrals in (10) can be readily evaluated and the resulting expansions for the electric and magnetic field vectors of the incident wave are listed in Appendix I.

### 3. *Multipole Expansions of the Scattered and Transmitted Fields*

In general, an arbitrarily polarized EM field involves both $E$-modes (TM) and $H$-modes (TE) and hence the scattered wave, in the domain exterior to the scatterer, can be expanded in terms of an infinite series of spherical vector wavefunctions as [22]

$$\begin{aligned} \mathbf{E}_s^{\parallel,\perp}(r, \theta, \phi) &= -\sum_{m=-\infty}^{\infty} \sum_{\substack{n=|m| \\ n\neq 0}}^{\infty} [a_{mn}^{\parallel,\perp}\mathbf{M}_{mn}^{(3)}(k_0 r) + b_{mn}^{\parallel,\perp}\mathbf{N}_{mn}^{(3)}(k_0 r)] \\ \mathbf{H}_s^{\parallel,\perp}(r, \theta, \phi) &= \frac{jk_0}{\omega\mu_0} \sum_{m=-\infty}^{\infty} \sum_{\substack{n=|m| \\ n\neq 0}}^{\infty} \\ &\qquad [a_{mn}^{\parallel,\perp}\mathbf{N}_{mn}^{(3)}(k_0 r) + b_{mn}^{\parallel,\perp}\mathbf{M}_{mn}^{(3)}(k_0 r)], \end{aligned} \tag{11}$$

where $(\mathbf{a}_{mn}^{\parallel,\perp}$ and $\mathbf{b}_{mn}^{\parallel,\perp})$ are the unknown expansion coefficients to be determined and

$$\begin{aligned} \mathbf{M}_{mn}(kr) &= f_n(kr) \exp(jm\phi) \\ &\qquad \left[\frac{jm}{\sin\theta} P_n^{|m|}(\cos\theta)\hat{\mathbf{a}}_\theta - \frac{dP_n^{|m|}(\cos\theta)}{d\theta}\hat{\mathbf{a}}_\phi\right] \\ \mathbf{N}_{mn}(kr) &= \exp(jm\phi)\left[n(n+1)\frac{f_n(kr)}{kr} P_n^{|m|}(\cos\theta)\hat{\mathbf{a}}_r \right. \\ &\qquad \left. + \hat{f}_n(kr)\left\{\frac{dP_n^{|m|}(\cos\theta)}{d\theta}\hat{\mathbf{a}}_\theta + j\frac{m}{\sin\theta} P_n^{|m|}(\cos\theta)\hat{\mathbf{a}}_\phi\right\}\right], \end{aligned} \tag{12}$$

where the generalized function $f_n(kr)$ is the appropriate kind of spherical Bessel functions (SBFs) of integer order $n$, $P_n^{|m|}(\cos\theta)$ denotes the associated Legendre functions of the first kind of degree $n$, and order $m$, where $P_n^{|m|}(\cos\theta) = 0$ for $n < m$ and $\hat{\mathbf{a}}_r$, $\hat{\mathbf{a}}_\theta$, and $\hat{\mathbf{a}}_\phi$ are orthonormal basis vectors associated with the spherical polar coordinate system $(r, \theta, \phi)$. The symbol $\hat{f}_n(kr)$ denotes the derivative of the product $kr\, f_n(kr)$ with respect to $kr$, divided by $kr$:

$$\hat{f}_n(kr) = \frac{f_n(kr)}{kr} + \frac{d}{dkr}[f_n(kr)]. \tag{13}$$

It should be remarked that complex linear combinations of the spherical vector wavefunctions, in the form of ("even" + $j$ "odd"), have been chosen in (12) similar to the form listed by Morrison and Cross [22]. The superscript 3 in (11) is used to denote that SBFs of the third kind; i.e., spherical Hankel functions (SHFs) of the first kind $h_n^{(1)}(k_0 r)$, are used for the radial functions.

Fields arising from the expansions given in (11) involve outgoing spherical waves at large distances form the origin and, hence, satisfy the radiation condition as stated in (4) since [27]

$$\lim_{r\to\infty} h_n^{(1)}(k_0 r) = (-j)^{n+1}\frac{\exp(jk_0 r)}{k_0 r}$$
$$\lim_{r\to\infty}\frac{1}{k_0 r}[k_0 r h_n^{(1)}(k_0 r)] = (-j)^n\frac{\exp(jk_0 r)}{k_0 r}. \tag{14}$$

In the general case of a dielectric core region, $f_n^{(1)} = j_n(k_1 r)$ are the only admissible radial-function solutions without a singularity at the origin, where $k_1 = \sqrt{\varepsilon_{r1}}k_0$ is the propagation constant inside the core region. Therefore, the following expansions are assumed for the fields internally induced in the core region:

$$\mathbf{E}_{f1}^{\parallel,\perp} = -\sum_{m=-\infty}^{\infty}\sum_{\substack{n\geq|m|\\ n\neq 0}}^{\infty}[c_{mn}^{\parallel,\perp}\mathbf{M}_{mn}^{(1)}(k_1 r) + d_{mn}^{\parallel,\perp}\mathbf{N}_{mn}^{(1)}(k_1 r)]$$
$$\mathbf{H}_{f1}^{\parallel,\perp} = \frac{jk_1}{\omega\mu_0}\sum_{m=-\infty}^{\infty}\sum_{\substack{n\geq|m|\\ n\neq 0}}^{\infty}[c_{mn}^{\parallel,\perp}\mathbf{N}_{mn}^{(1)}(k_1 r) + d_{mn}^{\parallel,\perp}\mathbf{M}_{mn}^{(1)}(k_1 r)]. \tag{15}$$

In the intermediate shell region, both the SBFs of the first kind $j_n(k_2 r)$, where $k_2 = \sqrt{\varepsilon_{r2}}k_0$ is the propagation constant in the shell region, and SBFs of the second kind, i.e., spherical Neumann functions $y_n(k_2 r)$ are well-behaved. Thus, it is necessary to write the general solution for the internal field induced in the shell region as a linear combination of them in the form

$$\mathbf{E}_{f2}^{\parallel,\perp} = -\sum_{m=-\infty}^{\infty}\sum_{\substack{n\geq|m|\\ n\neq 0}}^{\infty}[p_{mn}^{\parallel,\perp}\mathbf{M}_{mn}^{(1)}(k_2 r) + q_{mn}^{\parallel,\perp}\mathbf{M}_{mn}^{(2)}(k_2 r) + u_{mn}^{\parallel,\perp}\mathbf{N}_{mn}^{(1)}(k_2 r) + v_{mn}^{\parallel,\perp}\mathbf{N}_{mn}^{(2)}(k_2 r)]$$
$$\mathbf{H}_{f2}^{\parallel,\perp} = \frac{jk_2}{\omega\mu_0}\sum_{m=-\infty}^{\infty}\sum_{\substack{n\geq|m|\\ n\neq 0}}^{\infty}[p_{mn}^{\parallel,\perp}\mathbf{N}_{mn}^{(1)}(k_2 r) + q_{mn}^{\parallel,\perp}\mathbf{N}_{mn}^{(2)}(k_2 r) + u_{mn}^{\parallel,\perp}\mathbf{M}_{mn}^{(1)}(k_2 r) + v_{mn}^{\parallel,\perp}\mathbf{M}_{mn}^{(2)}(k_2 r)]. \tag{16}$$

The $r$, $\theta$, and $\phi$ components of the electric and magnetic field vectors of the scattered as well as the internal fields induced in the core and shell regions, which have been obtained by substituting the expressions for the spherical vector wavefunctions given in (12) into (11), (15), and (16), respectively, are listed in Appendix II.

### 4. *Imposing the Boundary Conditions*

Let $r_1$ and $r_2$ designate the length of the position vectors which are directed from the center of the scatterer to the inner and outer surfaces $S_1$ and $S_2$, respectively. They are defined by

$$r_1 = f_1(\theta), \quad r_2 = f_2(\theta) \tag{17}$$

for $0 \leq \theta \leq \pi$ and $0 \leq \phi \leq 2\pi$.

The geometrical form of the $S_1$ and $S_2$ surfaces, which enclose the core and outer shell regions, respectively, are then described by the following functions in spherical polar coordinates:

$$g_1(r, \theta) = r_1 - f_1(\theta) = 0$$
$$g_2(r, \theta) = r_2 - f_2(\theta) = 0. \tag{18}$$

The outward unit normal vectors $\hat{\mathbf{n}}_1$ and $\hat{\mathbf{n}}_2$ on the surfaces $S_1$ and $S_2$ are found from

$$\hat{\mathbf{n}}_1 = \nabla g_1(r, \theta) = \left(\hat{\mathbf{a}}_r - \frac{1}{r_1}\frac{df_1(\theta)}{d\theta}\hat{\mathbf{a}}_\theta\right)\Bigg/\sqrt{1+\left[\frac{1}{r_1}\frac{df_1(\theta)}{d\theta}\right]^2}$$
$$\hat{\mathbf{n}}_2 = \nabla g_2(r, \theta) = \left(\hat{\mathbf{a}}_r - \frac{1}{r_2}\frac{df_2(\theta)}{d\theta}\hat{\mathbf{a}}_\theta\right)\Bigg/\sqrt{1+\left[\frac{1}{r_2}\frac{df_2(\theta)}{d\theta}\right]^2}. \tag{19}$$

The boundary conditions, which require the continuity of the tangential components of the total electric and magnetic field vectors across the surfaces $S_1$ and $S_2$, can be expressed in terms of the following operator equations:

$$\left.\begin{aligned}\hat{\mathbf{n}}_1\times\{\mathbf{E}_{f2}^{\parallel,\perp}(\mathbf{r}) - \mathbf{E}_{f1}^{\parallel,\perp}(\mathbf{r})\} = 0\\ \hat{\mathbf{n}}_1\times\{\mathbf{H}_{f2}^{\parallel,\perp}(\mathbf{r}) - \mathbf{H}_{f1}^{\parallel,\perp}(\mathbf{r})\} = 0\end{aligned}\right\}\quad \mathbf{r}\in S_1 \tag{20}$$

$$\left.\begin{aligned}\hat{\mathbf{n}}_2\times\{\mathbf{E}_s^{\parallel,\perp}(\mathbf{r}) + \mathbf{E}_i^{\parallel,\perp}(\mathbf{r}) - \mathbf{E}_{f2}^{\parallel,\perp}(\mathbf{r})\} = 0\\ \hat{\mathbf{n}}_2\times\{\mathbf{H}_s^{\parallel,\perp}(\mathbf{r}) + \mathbf{H}_i^{\parallel,\perp}(\mathbf{r}) - \mathbf{H}_{f2}^{\parallel,\perp}(\mathbf{r})\} = 0\end{aligned}\right\}\quad \mathbf{r}\in S_2. \tag{21}$$

Furthermore, if the surface $S_1$ encloses a PC-core region, then $\mathbf{E}_{f1}^{\parallel,\perp}$ vanishes and the operator equations given in (20) reduce to

$$\hat{\mathbf{n}}_1\times\mathbf{E}_{f2}^{\parallel,\perp}(\mathbf{r}) = 0, \quad \mathbf{r}\in S_1 \tag{22}$$

When expressed in spherical polar components, each of the functional conditions represented by a single operator equation results in two independent scalar equations. Hence, the following eight equations for the $r$, $\theta$, and $\phi$ components of the field vectors, which are valid everywhere on $S_1$ and $S_2$, are obtained

$$
\begin{aligned}
&\mathbf{E}^{\parallel,\perp}_{i1,\phi}(r_1, \theta_1) = \mathbf{E}^{\parallel,\perp}_{i2,\phi}(r_1, \theta_1)\\
&\mathbf{H}^{\parallel,\perp}_{i1,\phi}(r_1, \theta_1) = \mathbf{H}^{\parallel,\perp}_{i2,\phi}(r_1, \theta_1)\\
&\mathbf{E}^{\parallel,\perp}_{i1,\phi}(r_1, \theta_1) + \frac{1}{r_1}\frac{df_1(\theta)}{d\theta}\mathbf{E}^{\parallel,\perp}_{i1,r}(r_1, \theta_1)\\
&\quad = \mathbf{E}^{\parallel,\perp}_{i2,\theta}(r_1, \theta_1) + \frac{1}{r_1}\frac{df_1(\theta)}{d\theta}\mathbf{E}^{\parallel,\perp}_{i2,r}(r_1, \theta_1) \qquad (23)\\
&\mathbf{H}^{\parallel,\perp}_{i1,\phi}(r_1, \theta_1) + \frac{1}{r_1}\frac{df_1(\theta)}{d\theta}\mathbf{H}^{\parallel,\perp}_{i1,r}(r_1, \theta_1)\\
&\quad = \mathbf{H}^{\parallel,\perp}_{i2,\theta}(r_1, \theta_1) + \frac{1}{r_1}\frac{df_1(\theta)}{d\theta}\mathbf{H}^{\parallel,\perp}_{i2,r}(r_1, \theta_1)
\end{aligned}
$$

and

$$
\begin{aligned}
&\mathbf{E}^{\parallel,\perp}_{i,\phi}(r_2, \theta_2) + \mathbf{E}^{\parallel,\perp}_{s,\phi}(r_2, \theta_2) = \mathbf{E}^{\parallel,\perp}_{i2,\phi}(r_2, \theta_2)\\
&\mathbf{H}^{\parallel,\perp}_{i,\phi}(r_2, \theta_2) + \mathbf{H}^{\parallel,\perp}_{s,\phi}(r_2, \theta_2) = \mathbf{H}^{\parallel,\perp}_{i2,\phi}(r_2, \theta_2)\\
&\mathbf{E}^{\parallel,\perp}_{i,\theta}(r_2, \theta_2) + \mathbf{E}^{\parallel,\perp}_{s,\theta}(r_2, \theta_2) + \frac{1}{r_2}\frac{df_2(\theta)}{d\theta}[\mathbf{E}^{\parallel,\perp}_{i,r}(r_2, \theta_2) + \mathbf{E}^{\parallel,\perp}_{s,r}(r_2, \theta_2)]\\
&\quad = \mathbf{E}^{\parallel,\perp}_{i2,\theta}(r_2, \theta_2) + \frac{1}{r_2}\frac{df_2(\theta)}{d\theta}\mathbf{E}^{\parallel,\perp}_{i2,r}(r_2, \theta_2)\\
&\mathbf{H}^{\parallel,\perp}_{i,\theta}(r_2, \theta_2) + \mathbf{H}^{\parallel,\perp}_{s,\theta}(r_2, \theta_2) + \frac{1}{r_2}\frac{df_2(\theta)}{d\theta}[\mathbf{H}^{\parallel,\perp}_{i,r}(r_2, \theta_2) + \mathbf{H}^{\parallel,\perp}_{s,r}(r_2, \theta_2)]\\
&\quad = \mathbf{H}^{\parallel,\perp}_{i2,\theta}(r_2, \theta_2) + \frac{1}{r_2}\frac{df_2(\theta)}{d\theta}\mathbf{H}^{\parallel,\perp}_{i2,r}(r_2, \theta_2). \qquad (24)
\end{aligned}
$$

In the special case of concentrically coated spheres, the orthogonality of the surface harmonics, $P_n^m(\cos\theta)\exp(jm\phi)$, can be invoked to provide analytical solutions for the set of eight unknown expansion coefficients from the system of equations given in (23) and (24). However, the general case of nonspherical bounding surfaces cannot be solved simply in the same manner since the infinite set of boundary-condition equations are coupled because of the angular dependence of the radial functions ($r_1$ and $r_2$ are functions of $\theta$).

Upon substituting the $r$, $\theta$, and $\phi$-components of the incident, scattered, and internal field vectors into (23) and (24), it turns out that all the terms in the resulting double sum, over the azimuthal and elevation modal indices, are multiplied by $\exp(jm\phi)$. The $\phi$-dependence of the boundary conditions can therefore be removed when these equations are multiplied by $\exp(-jm\phi)$ and integrated with respect to $\phi$ over the range from 0 to $2\pi$. Consequently, the azimuthal modal index is partially decoupled from the resultant system of boundary conditions, which for every $m$ mode (where $m = 0, 1, 2, \ldots$) can be written as shown in Appendix III.

In view of (I.1) to (I.4), (III.1), and (III.2) it can be shown that the following relationships exist among the unknown expansion coefficients for the two orthogonal polarizations of the incident wave:

$$
\begin{aligned}
&a^{\parallel}_{-mn} = -a^{\parallel}_{mn} \quad b^{\parallel}_{-mn} = b^{\parallel}_{mn}\\
&c^{\parallel}_{-mn} = -c^{\parallel}_{mn} \quad d^{\parallel}_{-mn} = d^{\parallel}_{mn}\\
&p^{\parallel}_{-mn} = -p^{\parallel}_{mn} \quad u^{\parallel}_{-mn} = u^{\parallel}_{mn}\\
&q^{\parallel}_{-mn} = -q^{\parallel}_{mn} \quad v^{\parallel}_{-mn} = v^{\parallel}_{mn}
\end{aligned} \qquad (25)
$$

and

$$
\begin{aligned}
&b^{\perp}_{-mn} = -b^{\perp}_{mn} \quad a^{\perp}_{-mn} = a^{\perp}_{mn}\\
&d^{\perp}_{-mn} = -d^{\perp}_{mn} \quad c^{\perp}_{-mn} = c^{\perp}_{mn}\\
&u^{\perp}_{-mn} = -u^{\perp}_{mn} \quad p^{\perp}_{-mn} = p^{\perp}_{mn}\\
&v^{\perp}_{-mn} = -v^{\perp}_{mn} \quad q^{\perp}_{-mn} = q^{\perp}_{mn}.
\end{aligned} \qquad (26)
$$

Therefore, only non-negative values of the azimuthal modal index are to be considered in the numerical implementation of the technique.

To this point the extent of the double summations in the expansions of the incident, scattered, and internal fields is assumed to be infinite. The azimuthal modal index $m$ varies from $-\infty$ to $\infty$, while for each $m$ the elevation modal index, $n$, runs for $|m|$ to $\infty$. Practically, only a finite number of terms is considered in the numerical analysis. The infinite modal summation over the elevation modal index is truncated at some finite index $n = N_0$ whose value is, in general, independent of $m$, while depending on the shape, composition and size of the scatterer. Thus, for a given azimuthal modal index $m$, we are left with $N_m$ unknown expansion coefficients, where $N_m = 8(N_0 - m + 1 - \delta_{m0})$, and $\delta_{m0}$ is the Kronecker delta.

We note here that the boundary-condition equations given in (III.1) and (III.2) are valid everywhere on the $S_1$ and $S_2$ surfaces. However, instead of enforcing the boundary conditions across the whole of the $S_1$ and $S_2$ surfaces, the equations required to solve for the $N_m$ unknowns are formulated by satisfying the boundary conditions, in the truncated system of (III.1), only at a discrete set of points. In our case of rotationally symmetric objects, the only necessary condition for the selection of matching points is that they should lead to independent equations. This can be satisfied by successively selecting $L_m$ boundary points along the $\theta$ direction, across the core and shell surfaces, which are given by $\theta_i$, $i = 1, L_m$, where $L_m \geq N_m/8$. The point-matching procedure mentioned above has to be carried out for all the number of significant azimuthal modes, which are necessary for convergence, starting from $m = 0$ up to $m = M_0$, where $M_0$ is not necessarily equal to $N_0$.

It should be pointed out that in this approach the boundary conditions are enforced only at a finite number of selected points on the $S_1$ and $S_2$ boundaries. The behavior of the fields at points not explicitly included in the point-matching procedure may be quite different from what is required by the conditions stated in (20) and (21).

For a given azimuthal modal index, the resultant system of boundary-condition equations can be written in matrix form as

$$\mathbf{A}_{ij}\mathbf{c}_j^{\parallel,\perp} = \mathbf{b}_i^{\parallel,\perp}. \tag{27}$$

Here, $\mathbf{A}_{ij}$ is an $8L_m$ by $N_m$ complex matrix and is referred to as the system matrix, the elements of which are explicit functions of the shape, size and dielectric properties of the core and shell regions as well as on the frequency and particular selection of matching points. The elements of $\mathbf{A}_{ij}$ are independent of the propagation and polarization directions of the incident wave. For each of the two orthogonal incident polarizations, the $N_m$-element column vector $\mathbf{c}_j^{\parallel,\perp}$ contains the unknown complex-valued expansion coefficients of the scattered and internal fields. The $8L_m$-element, complex column vector $\mathbf{b}_i^{\parallel,\perp}$ depends on the orientation, polarization, and frequency of the incident wave as well as the shape and size parameter of the outer shell surface.

For the purpose of reducing the dependence of the final solution on the particular selection of matching points, the boundary conditions indicated in (III.1) may be approximately satisfied by choosing $L_m > N_m/8$, and the expansion coefficients are then determined by minimizing the mean-squared error in the boundary fit over a set of points on the $S_1$ and $S_2$ surfaces, rather than over the entire surfaces. Thus, using the notation of vector norms, for each $m = 0, 1, \ldots, M_0$ our problem consists of minimizing the least-squares matrix equation $\min\|\mathbf{A}_{ij}\mathbf{c}_j^{\parallel,\perp} - \mathbf{b}_i^{\parallel,\perp}\|_2^2$, with respect to the vector of unknown expansion coefficients $\mathbf{c}_j^{\parallel,\perp}$, where the $\|\ \|_2$ symbol indicates the Euclidean 2-norm.

Since the matrix $\mathbf{A}_{ij}$ for a given scatterer in a fixed orientation is independent of both the incident polarization vector and the orientation of the scatterer with respect to the direction of propagation of the incident wave, once the matrix $\mathbf{A}_{ij}$ has been factored, the results obtained from either the Cholesky or the QR-decomposition for a particular orientation are written to a file for later use. For another scatterer orientation and/or incident polarization, it is relatively inexpensive to compute only the elements of the vector $\mathbf{b}_i^{\parallel,\perp}$ and to solve the resultant triangular system of equations as the factorization of the matrix $\mathbf{A}_{ij}$, which consumes most of the total computational time, has been accomplished. The efficiency of this strategy becomes apparent when the differential scattering characteristics of a given scatterer for various incident angles are required over different scattering planes.

### 5. *Definitions of Fundamental Scattering Parameters*

Once the approximate values of a finite number of the scattered field expansion coefficients $a_{mn}^{\parallel,\perp}$ and $b_{mn}^{\parallel,\perp}$ have been determined, the scattered field in the near and/or far-zone radiation regions and the various cross sections of interest may readily be evaluated. An elliptically polarized EM plane wave propagating in the $\mathbf{k}_i$ direction is assumed, where

$$\mathbf{k}_i = \mathbf{k}_0(\sin\theta_i\cos\phi_i\hat{\mathbf{a}}_x + \sin\theta_i\sin\phi_i\hat{\mathbf{a}}_y + \cos\theta_i\hat{\mathbf{a}}_z). \tag{28}$$

If the scattered wave is observed in the $\mathbf{k}_s$ direction, the incident and scattering directions will define a plane which is commonly referred to as the plane of scattering [28]. The electric field vector of the incident wave is resolved into two linearly polarized components, which are parallel and perpendicular to the scattering plane, respectively, as

$$\mathbf{E}_i = (E_i^{\parallel}\hat{\mathbf{a}}_i^{\parallel} + E_i^{\perp}\hat{\mathbf{a}}_i^{\perp})\exp(j\mathbf{k}_i\cdot\mathbf{r}), \tag{29}$$

where

$$\hat{\mathbf{a}}_i^{\parallel}\times\hat{\mathbf{a}}_i^{\perp} = \hat{\mathbf{k}}_i. \tag{30}$$

The orthonormal basis vectors $\hat{\mathbf{a}}_i^{\parallel}$ and $\hat{\mathbf{a}}_i^{\perp}$ are given by

$$\begin{aligned}\hat{\mathbf{a}}_i^{\parallel} &= \cos\theta_i(\cos\phi_i\hat{\mathbf{a}}_x + \sin\phi_i\hat{\mathbf{a}}_y) - \sin\theta_i\hat{\mathbf{a}}_z\\ \hat{\mathbf{a}}_i^{\perp} &= -\sin\phi_i\hat{\mathbf{a}}_x + \cos\phi_i\hat{\mathbf{a}}_y.\end{aligned} \tag{31}$$

At a distance $r > a^2/\lambda$, where $a$ is a typical maximum linear dimension of the scatterer, the scattered wave is approximately transverse ($\mathbf{E}_s\cdot\mathbf{k}_s \cong 0$) and behaves as a local plane wave having the form

$$\mathbf{E}_s = (E_s^{\parallel}\hat{\mathbf{a}}_s^{\parallel} + E_s^{\perp}\hat{\mathbf{a}}_s^{\perp})\exp(j\mathbf{k}_s\cdot\mathbf{r}), \tag{32}$$

where only terms in $r^{-1}$ are retained and

$$\mathbf{k}_s = \mathbf{k}_0(\sin\theta_s\cos\phi_s\hat{\mathbf{a}}_x + \sin\theta_s\sin\phi_s\hat{\mathbf{a}}_y + \cos\theta_s\hat{\mathbf{a}}_z). \tag{33}$$

The basis vectors $\hat{\mathbf{a}}_s^{\parallel}$ and $\hat{\mathbf{a}}_s^{\perp}$ are given by

$$\begin{aligned}\hat{\mathbf{a}}_s^{\parallel} &= \cos\theta_s(\cos\phi_s\hat{\mathbf{a}}_x + \sin\phi_s\hat{\mathbf{a}}_y) - \sin\theta_s\hat{\mathbf{a}}_z\\ \hat{\mathbf{a}}_s^{\perp} &= -\sin\phi_s\hat{\mathbf{a}}_x + \cos\phi_s\hat{\mathbf{a}}_y.\end{aligned} \tag{34}$$

The amplitude, phase, and polarization of the linearly polarized components of the far-field scattered wave can be described in terms of the corresponding components of the incident field vector by introducing the scattering function matrix which will assume the form

$$\begin{bmatrix}E_s^{\parallel}\\ E_s^{\perp}\end{bmatrix} = \frac{\exp(j\mathbf{k}_s\cdot\mathbf{r})}{r}\begin{bmatrix}f_{\parallel\parallel} & f_{\parallel\perp}\\ f_{\perp\parallel} & f_{\perp\perp}\end{bmatrix}\begin{bmatrix}E_i^{\parallel}\\ E_i^{\perp}\end{bmatrix}, \tag{35}$$

where $f_{ij}(\theta_s, \phi_s; \theta_i, \phi_i)$ is the ratio of the scattered wave component with polarization $i$ observed in the direction $(\theta_s, \phi_s)$, to the incident wave component, with polarization $j$, impinging in the direction $(\theta_i, \phi_i)$. With regard to the scatterer geometry shown in Fig. 1, the components of the far-field scattered wave are obtained from (11) using the asymptotic representation of the SHFs, as given in (14), which finally yields the expressions for the elements of the scattering function matrix,

$$f_{\parallel,\parallel} = \frac{1}{k_0}\sum_{m=0}^{M_0}\sum_{\substack{n\geq m\\ n\neq 0}}^{N_0}(-j)^{n+2}\varepsilon_m \left[\frac{m}{\sin\theta_s}P_n^m(\cos\theta_s)a_{mn}^{\parallel} + \frac{dP_n^m(\cos\theta_s)}{d\theta}b_{mn}^{\parallel}\right]\cos(m\phi_s)$$

$$f_{\parallel,\perp} = \frac{1}{k_0}\sum_{m=0}^{M_0}\sum_{\substack{n\geq m\\ n\neq 0}}^{N_0}(-j)^{n+1}\varepsilon_m \left[\frac{m}{\sin\theta_s}P_n^m(\cos\theta_s)a_{mn}^{\perp} + \frac{dP_n^m(\cos\theta_s)}{d\theta}b_{mn}^{\perp}\right]\sin(m\phi_s)$$

$$f_{\perp,\parallel} = \frac{1}{k_0}\sum_{m=0}^{M_0}\sum_{\substack{n\geq m\\ n\neq 0}}^{N_0}(-j)^{n+2}\varepsilon_m \left[\frac{dP_n^m(\cos\theta_s)}{d\theta}a_{mn}^{\parallel} + \frac{m}{\sin\theta_s}P_n^m(\cos\theta_s)b_{mn}^{\parallel}\right]\sin(m\phi_s)$$

$$f_{\perp,\perp} = \frac{1}{k_0}\sum_{m=0}^{M_0}\sum_{\substack{n\geq m\\ n\neq 0}}^{N_0}(-j)^{n+1}\varepsilon_m \left[\frac{dP_n^m(\cos\theta_s)}{d\theta}a_{mn}^{\perp} + \frac{m}{\sin\theta_s}P_n^m(\cos\theta_s)b_{mn}^{\perp}\right]\cos(m\phi_s), \tag{36}$$

where

$$\varepsilon_m = \begin{cases} 1, & m = 0 \\ 2, & m \geq 1 \end{cases} \quad \text{is the Neumann's factor.}$$

The scattering cross section, which is defined as the ratio of the total isotropically scattered power to the incident power flux density on a unit cross-sectional area of the scatterer, is evaluated from the following expression [22]:

$$Q_s^{\parallel,\perp} = \frac{4\pi}{k_0^2 E_i^{\parallel,\perp} E_i^{*\parallel,\perp}}\sum_{m=-\infty}^{\infty}\sum_{\substack{n\geq|m|\\ n\neq 0}}^{\infty}\frac{n(n+1)(n+|m|)!}{(2n+1)(n-|m|)!}[|a_{mn}^{\parallel,\perp}|^2 + |b_{mn}^{\parallel,\perp}|^2]. \tag{37}$$

The optical theorem [29] is used to evaluate the extinction cross section, which is the sum of the scattering and absorption cross sections, in terms of the imaginary part of the scattering amplitude function in the forward direction,

$$Q_e^{\parallel} = \frac{4\pi}{k_0}\,\mathrm{Im}[f_{\parallel,\parallel}(\mathbf{k}_i, \mathbf{k}_i)]$$
$$Q_e^{\perp} = \frac{4\pi}{k_0}\,\mathrm{Im}[f_{\perp,\perp}(\mathbf{k}_i, \mathbf{k}_i)]. \tag{38}$$

The absorption cross section is then determined from

$$Q_a^{\parallel,\perp} = Q_e^{\parallel,\perp} - Q_s^{\parallel,\perp}. \tag{39}$$

Other interesting parameters are the differential scattering cross section, in units of area per unit solid angle, which is defined for a unit incident electric field vector as the scattered power per unit solid angle in the direction $\mathbf{k}_s$, divided by the incident power flux density in the direction $\mathbf{k}_i$, and is given by [30]

$$\sigma_d^{\parallel}(\theta_s, \phi_s; \theta_i, \phi_i) = |\mathbf{E}_s^{\parallel}|^2$$
$$\sigma_d^{\perp}(\theta_s, \phi_s; \theta_i, \phi_i) = |\mathbf{E}_s^{\perp}|^2 \tag{40}$$

and the backscattering cross section,

$$Q_b^{\parallel,\perp} = 4\pi\sigma_d^{\parallel,\perp}(\pi - \theta_i, \pi + \phi_i; \theta_i, \phi_i). \tag{41}$$

### 6. *Transforming the Angular Scattering Pattern from Local to Principal Frames*

In many practical applications, the axes of the scattering object typically follow a prescribed orientation distribution and therefore it is essential to generalize the previously derived far-field scattering solution to deal with the case of an arbitrarily oriented scatterer. This is accomplished by introducing a second frame of reference, the principal frame $(x', y', z')$. It is often convenient to formulate the scattering problem in the principal frame, where the incident wave direction defines the $z'$-axis as shown in Fig. 2. The $x' - y'$ plane contains the incident electric

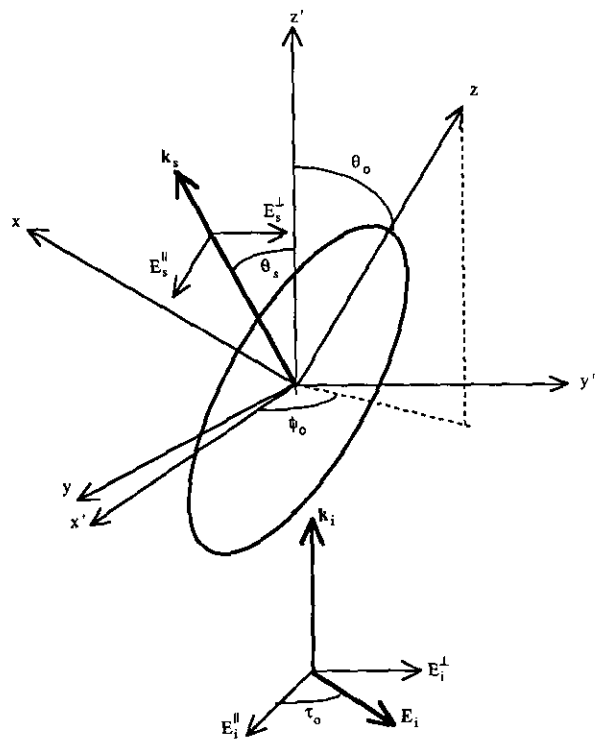


**FIG. 2.** Scattering geometry showing the local $(x, y, z)$ and principal$(x', y', z')$ frames. The direction of incidence is $z'$, the symmetry axis of the object is $z$ and is oriented at angles $(\theta_0, \phi_0)$. The incident field makes and angle $\tau_0$ with respect to the positive $x$-axis.

field vector which is, in general, inclined at an angle $\tau_0$ with respect to the $x'$-axis. The direction of the symmetry axis, which is specified in terms of the elevation and azimuthal angles $\theta_0$ and $\phi_0$, respectively, defines the orientation of the scatterer in the principal frame. It is required to determine the angular scattering pattern in the $x' - z'$ plane of the principal frame where $\phi_s'$ is either 0 or $\pi$, while $\theta_s'$ varies in general from 0 to $2\pi$. In establishing the following mathematical formulation, a procedure similar to the one given by Barber and Hill [30] will be followed.

The electric field vector of the incident wave is decomposed into two linearly polarized components, $\mathbf{E}_i^{\parallel'} = E_0 \cos \tau_0 \hat{\mathbf{a}}_{x'}$ and $\mathbf{E}_i^{\perp'} = E_0 \sin \tau_0 \hat{\mathbf{a}}_{y'}$.

The components ($\mathbf{E}_i^{\parallel'}$ and $\mathbf{E}_i^{\perp'}$) of the incident wave must be transformed to the local frame of the scatterer, where the burdensome operations of the scattering calculations are performed, before they are applied to the scattering matrix given in (35).

The position vector of a point $P$ with coordinates $(x, y, z)$, in the local frame, can be expressed in terms of the corresponding coordinates $(x', y', z')$ in the principal frame using the Eulerian angles of rotations which lead to the following transformation matrix, $[\mathbf{T}]$,

$$\begin{bmatrix} x \\ y \\ z \end{bmatrix} = [\mathbf{T}] \begin{bmatrix} x' \\ y' \\ z' \end{bmatrix},$$

where

$$[\mathbf{T}] = \begin{bmatrix} -\cos\phi_0 \cos\theta_0 & -\sin\phi_0 \cos\theta_0 & \sin\theta_0 \\ \sin\phi_0 & -\cos\phi_0 & 0 \\ \cos\phi_0 \sin\theta_0 & \sin\phi_0 \sin\theta_0 & \cos\theta_0 \end{bmatrix}. \quad (42)$$

The incident wave, the electric field vector of which lies in the $x' - y'$ plane, is described by the orthonormal basis vectors,

$$\mathbf{k}_i' = \hat{\mathbf{a}}_{z'}, \quad \hat{\mathbf{a}}_i^{\parallel'} = \hat{\mathbf{a}}_{x'}, \quad \hat{\mathbf{a}}_i^{\perp'} = \hat{\mathbf{a}}_{y'},$$

where $\hat{\mathbf{a}}_i^{\parallel'}$ and $\hat{\mathbf{a}}_i^{\perp'}$ are unit vectors along the polarization directions of the incident wave. The corresponding polarization vectors in the local frame ($\hat{\mathbf{a}}_i^{\parallel}, \hat{\mathbf{a}}_i^{\perp'}$) can be found from

$$\begin{aligned} \hat{\mathbf{a}}_i^{\perp'} &= \frac{\hat{\mathbf{a}}_z \times \hat{\mathbf{k}}_i'}{|\hat{\mathbf{a}}_z \times \hat{\mathbf{k}}_i'|} = \sin\phi_0 \hat{\mathbf{a}}_i^{\parallel'} - \cos\phi_0 \hat{\mathbf{a}}_i^{\perp'} \\ \hat{\mathbf{a}}_i^{\parallel} &= \hat{\mathbf{a}}_i^{\perp'} \times \hat{\mathbf{k}}_i' = -\cos\phi_0 \hat{\mathbf{a}}_i^{\parallel'} - \sin\phi_0 \hat{\mathbf{a}}_i^{\perp'}. \end{aligned} \quad (43)$$

Hence, the transformation of the components of the incident electric field vector from the principal frame to those in the local frame can be written in the form

$$\begin{bmatrix} E_i^{\parallel} \\ E_i^{\perp} \end{bmatrix} = \begin{bmatrix} -\cos\phi_0 & -\sin\phi_0 \\ \sin\phi_0 & -\cos\phi_0 \end{bmatrix} \begin{bmatrix} E_i^{\parallel'} \\ E_i^{\perp'} \end{bmatrix}. \quad (44)$$

The rectangular components of a unit vector $\mathbf{k}_s'$, in the direction of observation of the scattered wave, are given by

$$\begin{aligned} x' &= \sin\theta_s' \cos\phi_s' \\ z' &= \cos\theta_s'. \end{aligned} \quad (45)$$

The corresponding components in the local frame can be found from the transformation matrix in (42) as

$$\begin{aligned} x &= -\cos\phi_0 \cos\theta_0 \sin\theta_s' \cos\phi_s' + \sin\theta_0 \cos\theta_s' \\ y &= \sin\phi_0 \sin\theta_s' \cos\phi_s' \\ z &= \cos\phi_0 \sin\theta_0 \sin\theta_s' \cos\phi_s' + \cos\theta_0 \cos\theta_s'. \end{aligned} \quad (46)$$

The scattering angles $(\theta_s, \phi_s)$, required in the calculations of the elements of the scattering function matrix in (36), are found from

$$\begin{aligned} \theta_s &= \tan^{-1}(\sqrt{x^2 + y^2}/z) \\ \phi_s &= \tan^{-1}(y/x). \end{aligned} \quad (47)$$

With the fractional components of the incident electric field vector ($\mathbf{E}_i^{\parallel}$ and $\mathbf{E}_i^{\perp}$) and the scattering angles $(\theta_s, \phi_s)$ being determined, the final parameter required for the scattering calculations in the local frame is the angle of incidence $\theta_i$. Substituting $\theta_s' = \phi_s' = 0$ into (46), then it follows that $\theta_i = \theta_0$.

Once the elements of the scattering function matrix in (36) have been computed in the local frame, the components of the scattered electric field vector must be transformed back to the principal frame. In the far-field region, the transverse components of the scattered wave in the local frame and the associated orthonormal polarization vectors were given previously in (32) to (34). Similarly, the electric field vector of the scattered wave in the $x' - z'$ plane of the principal frame can be written as

$$\mathbf{E}_s' = E_s^{\parallel'} \hat{\mathbf{a}}_s^{\parallel'} + E_s^{\perp'} \hat{\mathbf{a}}_s^{\perp'}, \quad (48)$$

where

$$\begin{aligned} \hat{\mathbf{a}}_s^{\parallel'} &= \cos\theta_s' \cos\phi_s' \hat{\mathbf{a}}_{x'} - \sin\theta_s' \hat{\mathbf{a}}_{z'} \\ \hat{\mathbf{a}}_s^{\perp'} &= \cos\phi_s' \hat{\mathbf{a}}_{y'}. \end{aligned}$$

Note that $\mathbf{E}_s$ and $\mathbf{E}_s'$ have been specified relative to different basis vectors; however $\hat{\mathbf{a}}_{r'} = \hat{\mathbf{a}}_r$, since the two frames have a

common origin and, hence, the transverse polarization vectors $(\hat{\mathbf{a}}_s^{\parallel'}, \hat{\mathbf{a}}_s^{\perp'})$ and $(\hat{\mathbf{a}}_s^{\parallel}, \hat{\mathbf{a}}_s^{\perp})$ are all coplanar.

The desired transformation can be achieved easily by a 2D counterclockwise rotation about the radial vector $\hat{\mathbf{a}}_r$ as

$$\begin{bmatrix} E_s^{\parallel'} \\ E_s^{\perp'} \end{bmatrix} = \begin{bmatrix} \cos\gamma & \sin\gamma \\ -\sin\gamma & \cos\gamma \end{bmatrix} \begin{bmatrix} E_s^{\parallel} \\ E_s^{\perp} \end{bmatrix}, \tag{49}$$

where

$$\sin\gamma = \hat{\mathbf{a}}_s^{\parallel} \cdot \hat{\mathbf{a}}_s^{\perp'} = -\hat{\mathbf{a}}_s^{\perp'} \cdot \hat{\mathbf{a}}_s^{\parallel}$$
$$\cos\gamma = \hat{\mathbf{a}}_s^{\parallel'} \cdot \hat{\mathbf{a}}_s^{\parallel} = \hat{\mathbf{a}}_s^{\perp} \cdot \hat{\mathbf{a}}_s^{\perp'}.$$

In order to perform the dot products indicated above, $(\hat{\mathbf{a}}_s^{\parallel'}, \hat{\mathbf{a}}_s^{\perp'})$ are expressed in terms of $\hat{\mathbf{a}}_x$, $\hat{\mathbf{a}}_y$, and $\hat{\mathbf{a}}_z$ by substituting the inverse transformation $[\mathbf{T}]^{-1}$ to (49) which finally yields

$$\begin{aligned} \cos\gamma &= \cos\phi_s' \cos\phi_s \sin\phi_0 \cos\theta_0 - \cos\phi_s' \cos\phi_0 \cos\phi_s \\ \sin\gamma &= \cos\theta_s' \cos\phi_s' \sin\phi_s \cos\theta_0 \cos\phi_0 \\ &\quad + \sin\theta_s' \sin\phi_s \sin\theta_0 + \cos\theta_s' \cos\phi_s' \cos\phi_s \sin\phi_0. \end{aligned} \tag{50}$$

Thus, given a scatterer with orientation $\theta_0$, $\phi_0$ relative to the principal frame, the angular scattering pattern can be determined in the $x' - z'$ plane of the principal frame from

$$\begin{bmatrix} E_s^{\parallel'} \\ E_s^{\perp'} \end{bmatrix} = \begin{bmatrix} \cos\gamma & \sin\gamma \\ -\sin\gamma & \cos\gamma \end{bmatrix} \begin{bmatrix} f_{\parallel\parallel} & f_{\parallel\perp} \\ f_{\perp\parallel} & f_{\perp\perp} \end{bmatrix} \begin{bmatrix} -\cos\phi_0 & -\sin\phi_0 \\ \sin\phi_0 & -\cos\phi_0 \end{bmatrix} \begin{bmatrix} E_i^{\parallel'} \\ E_i^{\perp'} \end{bmatrix}. \tag{51}$$

## IV. SUMMARY

This paper presents the formulation of a computationally convenient procedure aimed towards extending the GPMT in the context of the analysis of 3D EM scattering and absorption characteristics of rotationally symmetric, PC, or dielectric obstacles embedded in axisymmetric, lossy, or lossless dielectric objects of arbitrary shape and arbitrarily disposed with respect to the direction of incidence of the impinging field. The method described here is capable of providing numerical results of controllable accuracy for two-layered objects of arbitrary geometrical surfaces for which analytical techniques, which may be obtained via the method of separation of variables, are either non-existing or analytically intractable particularly when the scatterer surface does not coincide with a constant coordinate surface in an orthogonal coordinate system in which the Helmholtz scalar wave equation is separable. Also, these solutions are essentially required when the scatterer dimensions are comparable to the wavelength of the incident radiation and where both the low-frequency Rayleigh approximation and high-frequency geometrical theory of diffraction techniques fail to yield reliable results. The particular choice of elementary spherical vector wavefunctions as basis functions has both advantages and disadvantages. Their chief advantage is that they represent a complete set of analytical solutions to Maxwell's equations since they are constructed from the exact eigenfunction modal solutions of the scalar wave equations, the individual elements of which are extensively tabulated. Other advantages are that they do not require extensive numerical computations and that they lead eventually to general and elegant computer codes which can be easily adapted for solving a large category of scatterer shapes. The relative disadvantages include the fact that scatterers with corners and/or edges cannot be tackled directly and that the method encounters obvious convergence problems for scatterers whose bounding surfaces depart significantly from a spherical shape such as for spheroids of moderately large ($\geq$4) and small ($\leq$0.4) axial ratios.

It should be mentioned that our GPMT matrix-equation formulation of the boundary-condition relations has been developed in such a manner that the elements of the overall system matrix are independent of the orientation of the scatterer as well as the polarization and incident directions of the incoming field vector. This leads to better computational efficiency and substantial saving in computer time and storage particularly for objects arbitrarily oriented with respect to the direction of propagation of an arbitrarily polarized incident field.

## APPENDIX I

$$\begin{aligned} E_{i,r}^{\parallel} &= -E_i^{\parallel} \exp(jk_0 r \cos\theta_i \cos\theta) \sum_{m=-\infty}^{\infty} j^m \\ &\quad [J_m(k_0 r \sin\theta_i \sin\theta) \sin\theta_i \cos\theta \\ &\quad + jJ_m'(k_0 r \sin\theta_i \sin\theta) \cos\theta_i \sin\theta] \exp(jm\phi) \\ E_{i,\theta}^{\parallel} &= E_i^{\parallel} \exp(jk_0 r \cos\theta_i \cos\theta) \sum_{m=-\infty}^{\infty} j^m \\ &\quad [J_m(k_0 r \sin\theta_i \sin\theta) \sin\theta_i \sin\theta \\ &\quad - jJ_m'(k_0 r \sin\theta_i \sin\theta) \cos\theta_i \cos\theta] \exp(jm\phi) \\ E_{i,\phi}^{\parallel} &= E_i^{\parallel} \cos\theta \exp(jk_0 r \cos\theta_i \cos\theta) \sum_{m=-\infty}^{\infty} j^m m \\ &\quad \frac{J_m(k_0 r \sin\theta_i \sin\theta)}{k_0 r \sin\theta_i \sin\theta} \exp(jm\phi) \end{aligned} \tag{I.1}$$

$$E_{i,r}^{\perp} = -E_i^{\perp} \sin\theta \exp(jk_0 r\cos\theta_i\cos\theta) \sum_{m=-\infty}^{\infty} j^m m \frac{J_m(k_0 r\sin\theta_i\sin\theta)}{k_0 r\sin\theta_i\sin\theta}\exp(jm\phi)$$

$$E_{i,\theta}^{\perp} = -E_i^{\perp} \cos\theta \exp(jk_0 r\cos\theta_i\cos\theta) \sum_{m=-\infty}^{\infty} j^m m \frac{J_m(k_0 r\sin\theta_i\sin\theta)}{k_0 r\sin\theta_i\sin\theta}\exp(jm\phi)$$

$$E_{i,\phi}^{\perp} = -E_i^{\perp} \exp(jk_0 r\cos\theta_i\cos\theta) \sum_{m=-\infty}^{\infty} j^{m+1} J_m'(k_0 r\sin\theta_i\sin\theta)\exp(jm\phi) \tag{I.2}$$

and

$$H_{i,r}^{\parallel} = \frac{k_0}{\omega\mu_0}\frac{E_i^{\parallel}}{E_i^{\perp}} E_{i,r}^{\perp}$$

$$H_{i,\theta}^{\parallel} = \frac{k_0}{\omega\mu_0}\frac{E_i^{\parallel}}{E_i^{\perp}} E_{i,\theta}^{\perp}$$

$$H_{i,\phi}^{\parallel} = \frac{k_0}{\omega\mu_0}\frac{E_i^{\parallel}}{E_i^{\perp}} E_{i,\phi}^{\perp} \tag{I.3}$$

$$H_{i,r}^{\perp} = \frac{-k_0}{\omega\mu_0}\frac{E_i^{\perp}}{E_i^{\parallel}} E_{i,r}^{\parallel}$$

$$H_{i,\theta}^{\perp} = \frac{-k_0}{\omega\mu_0}\frac{E_i^{\perp}}{E_i^{\parallel}} E_{i,\theta}^{\parallel}$$

$$H_{i,\phi}^{\perp} = \frac{-k_0}{\omega\mu_0}\frac{E_i^{\perp}}{E_i^{\parallel}} E_{i,\phi}^{\parallel}, \tag{I.4}$$

where $J_m$ is the ordinary Bessel function of the first kind of order $m$, the prime denotes derivative with respect to the argument and an additional subscript has been attached to denote the $r$, $\theta$, and $\phi$ components of the corresponding field vectors.

For the particular case of an incident plane wave propagating along the axis of symmetry of the scatterer, all of the azimuthal modes vanish except for $m = \pm 1$. Special attention should be devoted to the evaluation of the incident field expansions given in (I.1) and (I.2) due to the singular behavior of the functions $J_m(x)/x$ and $J_m'(x)$ when $x = 0$. The resulting expressions are found to be

$$E_{i,r}^{\parallel} = E_i^{\parallel}\sin\theta\cos\phi\exp(jk_0 r\cos\theta)$$
$$E_{i,\theta}^{\parallel} = E_i^{\parallel}\cos\theta\cos\phi\exp(jk_0 r\cos\theta) \tag{I.5}$$
$$E_{i,\phi}^{\parallel} = -E_i^{\parallel}\sin\phi\exp(jk_0 r\cos\theta)$$

and

$$E_{i,r}^{\perp} = E_i^{\perp}\sin\theta\sin\phi\exp(jk_0 r\cos\theta)$$
$$E_{i,\theta}^{\perp} = E_i^{\perp}\cos\theta\sin\phi\exp(jk_0 r\cos\theta) \tag{I.6}$$
$$E_{i,\phi}^{\perp} = E_i^{\perp}\cos\phi\exp(jk_0 r\cos\theta).$$

## APPENDIX II

$$E_{s,r}^{\parallel,\perp} = -\sum_{m=-\infty}^{\infty}\sum_{\substack{n\geq|m|\\ n\neq 0}}^{\infty} b_{mn}^{\parallel,\perp} n(n+1)\frac{h_n^{(1)}(k_0 r)}{k_0 r} P_n^{|m|}(\cos\theta)\exp(jm\phi)$$

$$E_{s,r}^{\parallel,\perp} = -\sum_{m=-\infty}^{\infty}\sum_{\substack{n\geq|m|\\ n\neq 0}}^{\infty}\left\{jma_{mn}^{\parallel,\perp} h_n^{(1)}(k_0 r)\frac{P_n^{|m|}(\cos\theta)}{\sin\theta} + b_{mn}^{\parallel,\perp}\hat{f}_n^{(3)}(k_0 r)\frac{dP_n^{|m|}(\cos\theta)}{d\theta}\right\}\exp(jm\phi)$$

$$E_{s,\phi}^{\parallel,\perp} = \sum_{m=-\infty}^{\infty}\sum_{\substack{n\geq|m|\\ n\neq 0}}^{\infty}\left\{a_{mn}^{\parallel,\perp} h_n^{(1)}(k_0 r)\frac{dP_n^{|m|}(\cos\theta)}{d\theta} - jmb_{mn}^{\parallel,\perp}\hat{f}_n^{(3)}(k_0 r)\frac{P_n^{|m|}(\cos\theta)}{\sin\theta}\right\}\exp(jm\phi) \tag{II.1}$$

$$H_{s,r}^{\parallel,\perp} = \frac{jk_0}{\omega\mu_0}\sum_{m=-\infty}^{\infty}\sum_{\substack{n\geq|m|\\ n\neq 0}}^{\infty} a_{mn}^{\parallel,\perp} n(n+1)\frac{h_n^{(1)}(k_0 r)}{k_0 r} P_n^{|m|}(\cos\theta)\exp(jm\phi)$$

$$H_{s,\theta}^{\parallel,\perp} = \frac{jk_0}{\omega\mu_0}\sum_{m=-\infty}^{\infty}\sum_{\substack{n\geq|m|\\ n\neq 0}}^{\infty}\left\{a_{mn}^{\parallel,\perp}\hat{f}_n^{(3)}(k_0 r)\frac{dP_n^{|m|}(\cos\theta)}{d\theta} + jmb_{mn}^{\parallel,\perp} h_n^{(1)}(k_0 r)\frac{P_n^{|m|}(\cos\theta)}{\sin\theta}\right\}\exp(jm\phi)$$

$$H_{s,\phi}^{\parallel,\perp} = \frac{jk_0}{\omega\mu_0}\sum_{m=-\infty}^{\infty}\sum_{\substack{n\geq|m|\\ n\neq 0}}^{\infty}\left\{jma_{mn}^{\parallel,\perp}\hat{f}_n^{(3)}(k_0 r)\frac{P_n^{|m|}(\cos\theta)}{\sin\theta} - b_{mn}^{\parallel,\perp} h_n^{(1)}(k_0 r)\frac{dP_n^{|m|}(\cos\theta)}{d\theta}\right\}\exp(jm\phi). \tag{II.2}$$

The $r$, $\theta$, and $\phi$ components of the internal field induced in the core region are similar to those listed in (II.1) and (II.2) with $k_1$, $j_n(k_1 r)$, $c_{mn}^{\parallel,\perp}$, and $d_{mn}^{\parallel,\perp}$ replacing $k_0$, $h_n^{(1)}(k_0 r)$, $a_{nm}^{\parallel,\perp}$, and $b_{mn}^{\parallel,\perp}$, respectively. For the shell region the field components are given by

$$E^{\parallel,\perp}_{12,r} = -\sum_{m=-\infty}^{\infty}\sum_{\substack{n\geq|m|\\ n\neq 0}}^{\infty} n(n+1)P_n^{|m|}(\cos\theta)$$
$$\left\{u^{\parallel,\perp}_{mn}\frac{j_n(k_2r)}{k_2r} + v^{\parallel,\perp}_{mn}\frac{y_n(k_2r)}{k_2r}\right\}\exp(jm\phi)$$

$$E^{\parallel,\perp}_{12,\theta} = -\sum_{m=-\infty}^{\infty}\sum_{n\geq|m|}^{\infty}\left[jm\frac{P_n^{|m|}(\cos\theta)}{\sin\theta}\{p^{\parallel,\perp}_{mn}j_n(k_2r) + q^{\parallel,\perp}_{mn}y_n(k_2r)\}\right.$$
$$\left. + \frac{dP_n^{|m|}(\cos\theta)}{d\theta}\{u^{\parallel,\perp}_{mn}\hat{f}_n^{(1)}(k_2r) + v^{\parallel,\perp}_{mn}\hat{f}_n^{(2)}(k_2r)\}\right]\exp(jm\phi)$$

$$E^{\parallel,\perp}_{12,\phi} = \sum_{m=-\infty}^{\infty}\sum_{\substack{n\geq|m|\\ n\neq 0}}^{\infty}\left[\frac{dP_n^{|m|}(\cos\theta)}{d\theta}\{p^{\parallel,\perp}_{mn}j_n(k_2r) + q^{\parallel,\perp}_{mn}y_n(k_2r)\}\right.$$
$$\left. - jm\frac{P_n^{|m|}(\cos\theta)}{\sin\theta}\{u^{\parallel,\perp}_{mn}\hat{f}_n^{(1)}(k_2r) + v^{\parallel,\perp}_{mn}\hat{f}_n^{(2)}(k_2r)\}\right]\exp(jm\phi) \tag{II.3}$$

and

$$H^{\parallel,\perp}_{12,r} = \frac{jk_2}{\omega\mu_0}\sum_{m=-\infty}^{\infty}\sum_{\substack{n\geq|m|\\ n\neq 0}}^{\infty} n(n+1)P_n^{|m|}(\cos\theta)$$
$$\left\{p^{\parallel,\perp}_{mn}\frac{j_n(k_2r)}{k_2r} + q^{\parallel,\perp}_{mn}\frac{y_n(k_2r)}{k_2r}\right\}\exp(jm\phi)$$

$$H^{\parallel,\perp}_{12,\theta} = \frac{jk_2}{\omega\mu_0}\sum_{m=-\infty}^{\infty}\sum_{\substack{n\geq|m|\\ n\neq 0}}^{\infty}\left[\frac{dP_n^{|m|}(\cos\theta)}{d\theta}\{p^{\parallel,\perp}_{mn}\hat{f}_n^{(1)}(k_2r) + q^{\parallel,\perp}_{mn}\hat{f}_n^{(2)}(k_2r)\}\right.$$
$$\left. + jm\frac{P_n^{|m|}(\cos\theta)}{\sin\theta}\{u^{\parallel,\perp}_{mn}j_n(k_2r) + v^{\parallel,\perp}_{mn}y_n(k_2r)\}\right]\exp(jm\phi)$$

$$H^{\parallel,\perp}_{12,\phi} = \frac{jk_2}{\omega\mu_0}\sum_{m=-\infty}^{\infty}\sum_{\substack{n\geq|m|\\ n\neq 0}}^{\infty}\left[jm\frac{P_n^{|m|}(\cos\theta)}{\sin\theta}\right.$$
$$\{p^{\parallel,\perp}_{mn}\hat{f}_n^{(1)}(k_2r) + q^{\parallel,\perp}_{mn}\hat{f}_n^{(2)}(k_2r)\}$$
$$\left. - \frac{dP_n^{|m|}(\cos\theta)}{d\theta}\{u^{\parallel,\perp}_{mn}j_n(k_2r) + v^{\parallel,\perp}_{mn}y_n(k_2r)\}\right]\exp(jm\phi). \tag{II.4}$$

## APPENDIX III

$$\sum_{\substack{n\geq|m|\\ n\neq 0}} C_{1,mn}c^{\parallel,\perp}_{mn} + D_{1,mn}d^{\parallel,\perp}_{mn} + P_{1,mn}p^{\parallel,\perp}_{mn} + Q_{1,mn}q^{\parallel,\perp}_{mn}$$
$$+ U_{1,mn}u^{\parallel,\perp}_{mn} + V_{1,mn}v^{\parallel,\perp}_{mn} = 0$$

$$\sum_{\substack{n\geq|m|\\ n\neq 0}} \sqrt{\varepsilon_{r1}}(D_{1,mn}c^{\parallel,\perp}_{mn} + C_{1,mn}d^{\parallel,\perp}_{mn}) + \sqrt{\varepsilon_{r2}}(U_{1,mn}p^{\parallel,\perp}_{mn} + V_{1,mn}q^{\parallel,\perp}_{mn}$$
$$+ P_{1,mn}u^{\parallel,\perp}_{mn} + Q_{1,mn}v^{\parallel,\perp}_{mn}) = 0$$

$$\sum_{\substack{n\geq|m|\\ n\neq 0}} C_{3,mn}c^{\parallel,\perp}_{mn} + D_{3,mn}d^{\parallel,\perp}_{mn} + P_{3,mn}p^{\parallel,\perp}_{mn} + Q_{3,mn}q^{\parallel,\perp}_{mn} + U_{3,mn}u^{\parallel,\perp}_{mn}$$
$$+ V_{3,mn}v^{\parallel,\perp}_{mn} = 0$$

$$\sum_{\substack{n\geq|m|\\ n\neq 0}} \sqrt{\varepsilon_{r1}}(D_{3,mn}c^{\parallel,\perp}_{mn} + C_{3,mn}d^{\parallel,\perp}_{mn}) + \sqrt{\varepsilon_{r2}}(U_{3,mn}p^{\parallel,\perp}_{mn} + V_{3,mn}q^{\parallel,\perp}_{mn}$$
$$+ P_{3,mn}u^{\parallel,\perp}_{mn} + Q_{3,mn}v^{\parallel,\perp}_{mn}) = 0$$

and

$$\sum_{\substack{n\geq|m|\\ n\neq 0}} A_{5,mn}a^{\parallel,\perp}_{mn} + B_{5,mn}b^{\parallel,\perp}_{mn} + P_{5,mn}p^{\parallel,\perp}_{mn} + Q_{5,mn}q^{\parallel,\perp}_{mn}$$
$$+ U_{5,mn}u^{\parallel,\perp}_{mn} + V_{5,mn}v^{\parallel,\perp}_{mn} = R^{\parallel,\perp}_{5,m}$$
$$\sum_{\substack{n\geq m\\ n\neq 0}} B_{5,mn}a^{\parallel,\perp}_{mn} + A_{5,mn}b^{\parallel,\perp}_{mn} + \sqrt{\varepsilon_{r2}}(U_{5,mn}p^{\parallel,\perp}_{mn} + V_{5,mn}q^{\parallel,\perp}_{mn}$$
$$+ P_{5,mn}u^{\parallel,\perp}_{mn} + Q_{5,mn}v^{\parallel,\perp}_{mn}) = R^{\parallel,\perp}_{6,m}$$
$$\sum_{\substack{n\geq|m|\\ n\neq 0}} A_{7,mn}a^{\parallel,\perp}_{mn} + B_{7,mn}b^{\parallel,\perp}_{mn} + P_{7,mn}p^{\parallel,\perp}_{mn} + Q_{7,mn}q^{\parallel,\perp}_{mn}$$
$$+ U_{7,mn}u^{\parallel,\perp}_{mn} + V_{7,mn}v^{\parallel,\perp}_{mn} = R^{\parallel,\perp}_{7,m}$$
$$\sum_{\substack{n\geq|m|\\ n\neq 0}} B_{7,mn}a^{\parallel,\perp}_{mn} + A_{7,mn}b^{\parallel,\perp}_{mn} + \sqrt{\varepsilon_{r2}}(U_{7,mn}p^{\parallel,\perp}_{mn} + V_{7,mn}q^{\parallel,\perp}_{mn}$$
$$+ P_{7,mn}u^{\parallel,\perp}_{mn} + Q_{7,mn}v^{\parallel,\perp}_{mn}) = R^{\parallel,\perp}_{8,m}, \tag{III.1}$$

where

$$C_{1mn} = j_n(k_1r_1)\frac{dP_n^{|m|}(\cos\theta)}{d\theta}$$

$$D_{1mn} = -jm\hat{f}_n^{(1)}(k_1r_1)\frac{P_n^{|m|}(\cos\theta)}{\sin\theta}$$

$$P_{1mn} = -j_n(k_2r_1)\frac{dP_n^{|m|}(\cos\theta)}{d\theta}$$

$$Q_{1mn} = -y_n(k_2r_1)\frac{dP_n^{|m|}(\cos\theta)}{d\theta}$$

$$U_{1,mn} = jm\hat{f}_n^{(1)}(k_2r_1)\frac{P_n^{|m|}(\cos\theta)}{\sin\theta}$$

$$V_{1,mn} = jm\hat{f}_n^{(2)}(k_2r_1)\frac{P_n^{|m|}(\cos\theta)}{\sin\theta}$$

$$C_{3,mn} = -jmj_n(k_1r_1)\frac{P_n^{|m|}(\cos\theta)}{\sin\theta}$$

$$D_{3,mn} = -\hat{f}_n^{(1)}(k_1 r_1)\frac{dP_n^{|m|}(\cos\theta)}{d\theta} + \frac{1}{r_1}\frac{df_1(\theta)}{d\theta} n(n+1)\frac{j_n(k_1 r_1)}{k_1 r_1} P_n^{|m|}(\cos\theta)$$

$$P_{3,mn} = jmj_n(k_2 r_1)\frac{P_n^{|m|}(\cos\theta)}{\sin\theta}$$

$$U_{3,mn} = \hat{f}_n^{(1)}(k_2 r_1)\frac{dP_n^{|m|}(\cos\theta)}{d\theta} + \frac{1}{r_1}\frac{df_1(\theta)}{d\theta} n(n+1)\frac{j_n(k_2 r_1)}{k_2 r_1} P_n^{|m|}(\cos\theta)$$

$$V_{3,mn} = \hat{f}_n^{(2)}(k_2 r_1)\frac{dP_n^{|m|}(\cos\theta)}{d\theta} + \frac{1}{r_1}\frac{df_1(\theta)}{d\theta} n(n+1)\frac{y_n(k_2 r_1)}{k_2 r_1} P_n^{|m|}(\cos\theta)$$

$$A_{5,mn} = h_n^{(1)}(k_0 r_2)\frac{dP_n^{|m|}(\cos\theta)}{d\theta}$$

$$B_{5,mn} = -jm\hat{f}_n^{(3)}(k_0 r_2)\frac{P_n^{|m|}(\cos\theta)}{\sin\theta}$$

$$P_{5,mn} = -j_n(k_2 r_2)\frac{dP_n^{|m|}(\cos\theta)}{d\theta}$$

$$Q_{5,mn} = -y_n(k_2 r_2)\frac{dP_n^{|m|}(\cos\theta)}{d\theta}$$

$$U_{5,mn} = -jm\hat{f}_n^{(1)}(k_2 r_2)\frac{P_n^{|m|}(\cos\theta)}{\sin\theta}$$

$$V_{5,mn} = jm\hat{f}_n^{(2)}(k_2 r_2)\frac{P_n^{|m|}(\cos\theta)}{\sin\theta}$$

$$A_{7,mn} = -jmh_n^{(1)}(k_0 r_2)\frac{P_n^{|m|}(\cos\theta)}{\sin\theta}$$

$$B_{7,mn} = -\left[\hat{f}_n^{(3)}(k_0 r_2)\frac{dP_n^{|m|}(\cos\theta)}{d\theta} + \frac{1}{r_2}\frac{df_2(\theta)}{d\theta} n(n+1)\frac{h_n^{(1)}(k_0 r_2)}{k_0 r_2} P_n^{|m|}(\cos\theta)\right]$$

$$P_{7,mn} = jmj_n(k_2 r_2)\frac{P_n^{|m|}(\cos\theta)}{\sin\theta}$$

$$Q_{7,mn} = jmy_n(k_2 r_2)\frac{P_n^{|m|}(\cos\theta)}{\sin\theta}$$

$$U_{7,mn} = \hat{f}_n^{(1)}(k_2 r_2)\frac{dP_n^{|m|}(\cos\theta)}{d\theta} + \frac{1}{r_2}\frac{df_2(\theta)}{d\theta} n(n+1) P_n^{|m|}(\cos\theta)$$

$$V_{7,mn} = \hat{f}_n^{(2)}(k_2 r_2)\frac{dP_n^{|m|}(\cos\theta)}{d\theta} + \frac{1}{r_2}\frac{df_2(\theta)}{d\theta} n(n+1)\frac{y_n(k_2 r_2)}{k_2 r_2}$$

$$R_{6,m}^{\parallel} = j^{m+2} E_i^{\parallel} J_m'(k_0 r_2 \sin\theta_i \sin\theta)\exp(jk_0 r_2 \cos\theta_i \cos\theta)$$

$$R_{5,m}^{\perp} = j^{m+1} E_i^{\perp} J_m'(k_0 r_2 \sin\theta_i \sin\theta)\exp(jk_0 r_2 \cos\theta_i \cos\theta)$$

$$R_{6,m}^{\parallel} = j^{m+2} E_i^{\parallel} J_m'(k_0 r_2 \sin\theta_i \sin\theta)\exp(jk_0 r_2 \cos\theta_i \cos\theta)$$

$$R_{6,m}^{\perp} = j^{m+1} E_i^{\perp} \cos\theta_i \frac{mJ_m(k_0 r_2 \sin\theta_i \sin\theta)}{k_0 r_2 \sin\theta_i \sin\theta}\exp(jk_0 r_2 \cos\theta_i \cos\theta)$$

$$R_{7,m}^{\parallel} = -j^m E_i^{\parallel}[J_m(k_0 r_2 \sin\theta_i \sin\theta)\sin\theta_i \sin\theta - J_m'(k_0 r_2 \sin\theta_i \sin\theta)\cos\theta_i \cos\theta - \frac{1}{r_2}\frac{df_2(\theta)}{d\theta}\{J_m(k_0 r_2 \sin\theta_i \sin\theta)\sin\theta_i \cos\theta + jJ_m'(k_0 r_2 \sin\theta_i \sin\theta)\cos\theta_i \sin\theta\} \exp(jk_0 r_2 \cos\theta_i \cos\theta)$$

$$R_{7,m}^{\perp} = j^m E_i^{\perp}\frac{mJ_m(k_0 r_2 \sin\theta_i \sin\theta)}{k_0 r_2 \sin\theta_i \sin\theta}\left(\cos\theta + \frac{1}{r_2}\frac{df_2(\theta)}{d\theta}\sin\theta\right)\exp(jk_0 r_2 \cos\theta_i \cos\theta)$$

$$R_{8,m}^{\parallel} = j^{m+1} E_i^{\parallel}\frac{mJ_m(k_0 r_2 \sin\theta_i \sin\theta)}{k_0 r_2 \sin\theta_i \sin\theta}\left(\cos\theta + \frac{1}{r_2}\frac{df_2(\theta)}{d\theta}\sin\theta\right)\exp(jk_0 r_2 \cos\theta_i \cos\theta)$$

$$R_{8,m}^{\perp} = j^{m+1} E_i^{\perp}\left[J_m(k_0 r_2 \sin\theta_i \sin\theta)\sin\theta_i \sin\theta - jJ_m'(k_0 r_2 \sin\theta_i \sin\theta)\cos\theta_i \cos\theta - \frac{1}{r_2}\frac{df_2(\theta)}{d\theta}\{J_m(k_0 r_2 \sin\theta_i \sin\theta)\sin\theta_i \cos\theta + jJ_m'(k_0 r_2 \sin\theta_i \sin\theta)\cos\theta_i \sin\theta\}\right] \exp(jk_0 r_2 \cos\theta_i \cos\theta). \quad \text{(III.2)}$$

## REFERENCES


1. A. L. Aden and M. Kerker, *J. Appl. Phys.* **22,** 1242 (1951).
2. P. C. Waterman, *Proc. IEEE* **53,** 805 (1965).
3. P. C. Waterman, *Alta Freq.* **38,** 348 (1969).
4. Bo. Peterson and S. Ström, *Phys. Rev. D* **180,** 2670 (1974).

5. V. N. Bringi and T. A. Seliga, *IEEE Trans. Antennas Propagat.* **AP25,** 575 (1979).
6. V. N. Bringi and T. A. Seliga, *Ann. Telecom.* **32,** 392 (1977).
7. E. M. Purcell and C. R. Pennypacker, *Astrophys. J.* **186,** 705 (1973).
8. S. D. Druger, M. Kerker, D. S. Wang, and D. D. Cooke, *Appl. Opt.* **18,** 3888 (1979).
9. R. J. Pogorzelski, *IEEE Trans. Antennas Propagat.* **AP-26,** 616 (1978).
10. J. R. Mautz and R. F. Harrington, *Appl. Sci. Res.* **20,** 405 (1969).
11. L. N. Medgyesi-Mitschang and C. Eftimitu, *Appl. Phys.* **19,** 275 (1979).
12. D. S. Wang and P. W. Barber, *Appl. Opt.* **18,** 1190 (1979).
13. A. A. Kishk and L. Shafai, *IEE Proc.* **133,** H, 227 (1986).
14. M. A. Morgan, C. H. Chen, S. C. Hill, and P. W. Barber, *Wave Motion* **6,** 91 (1984).
15. X. Yuan, D. R. Lynch, and J. W. Strohbehn, *IEEE Trans. Antennas Propagat.* **AP-38,** 386 (1990).
16. A. R. Sebak and B. P. Sinha, *IEEE Trans. Antennas Propagat.* **AP-40,** 268 (1992).
17. H. M. Al-Rizzo and J. M. Tranquilla, *J. Comput. Phys.* **119** (1995).
18. C. R. Mullin, R. Sandburg, and C. O. Velline, *IEEE Trans. Antennas Propagat.* **AP-12,** 141 (1965).
19. H. Y. Yee, *IEEE Trans. Antennas Propagat.* **AP-12,** 822 (1965).
20. Y. Mushiake, *J. Appl. Phys.* **27,** 1549 (1956).
21. T. Oguchi and Y. Hosoya, *J. Radio Res. Lab. Japan* **21,** 191 (1974).
22. J. A. Morrison and M. J. Cross, *Bell Syst. Tech. J.* **53,** 955 (1974).
23. C. Hafner and N. Kuster, *Radio Sci.* **26,** 291 (1991).
24. A. C. Ludwig, *IEEE Trans. Antennas Propagat.* **AP-34,** 857 (1986).
25. K. Joo and M. F. Iskander, *IEEE Trans. Antennas Propagat.* **AP-38,** 1483 (1990).
26. R. S. Elliot, *Antenna Theory and Design* (Prentice–Hall, Englewood Cliffs, NJ, 1981).
27. J. A. Stratton, *Electromagnetic Theory* (McGraw–Hill, New York, 1941).
28. A. Ishimaru, *Wave Propagation and Scattering in Random Media*, Vols. I, II (Academic Press, New York, 1978).
29. M. Born and E. Wolf, *Principles of Optics* (Pergamon, New York, 1981).
30. P. W. Barber and S. C. Hill, *Light Scattering by Particles: Computational Methods* (World Scientific, Princeton, NJ, 1990).